Analysis and Evaluation of Three-Stage Twisty Octapole Field Electromagnetic Launcher

Zhu Yingwei, Wang Yu, Chen Weirong, Yan Zhongming, and Li Haitao

***Abstract*—In this paper, we propose an improved launch mode called multistage twisty multipole electromagnetic launcher. The twisty multipole magnetic field configuration is resolved, and the group power supply module is considered. The induced eddy current of the projectile is considered, and the analysis of electromagnetic force and torque has been performed. A full 3-D transient motion simulation with multiple degrees of freedom is carried on the three-stage twisty octapole field electromagnetic launcher. The simulation results indicate that the magnetic torque of rotational motion is impressively large and the transverse displacement of the projectile is much little. The torsion option of multistage pole coils makes little influence on axial acceleration force and exit velocity comparing with the appositional configuration. The theoretical analysis and numerical simulations indicate that the projectile is accelerated with spinning motion about its axis which could keep the projectile fly stability. We suggest this launch mode could be applied in the evacuated tube transportation vehicle.**

***Index Terms*—Coilguns, multipole field electromagnetic launcher, spinning stability, twisty traveling magnetic wave.**

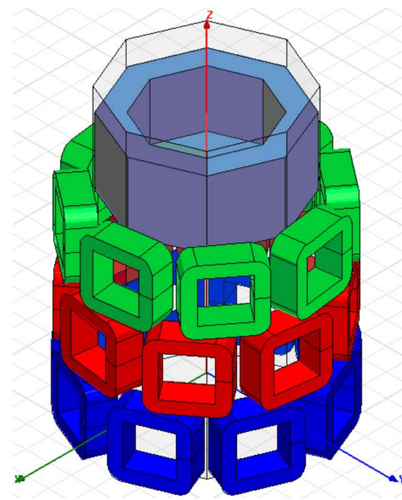

Fig. 1. Three-stage twisty octapole field electromagnetic launcher.

I. Introduction

OVER THE last three decades, the world continues a broad and deep research to develop electromagnetic launch technology [1]. Pulsed power supply using superconducting magnetic cable energy storage system is capable of providing current of 6 MA to railgun barrels. Some projectiles' exit velocities of more than 6 km/s have been achieved, and muzzle energies in excess of 10 MJ have been repeatedly demonstrated with railguns [2]–[6]. The conventional coilguns with coaxial coils, including the brush-fed and induction-type launcher, could reduce the power current requirements and remove the mechanical and electrical contact. However, all the linear coaxial coilguns have greater radial component of electromagnetic force that leads to a decrease in axial force used to accelerate the projectile to high speed.

The multipole field electromagnetic launch mode is proposed under the exploring for new acceleration magnetic configuration, and its principle feasibility comes from the linear induction motor and the reconnection gun [7]. In a recent paper, the launch mode and circuit equation of appositional electromagnetic launcher are discussed in theory, and the single stage of octapole field electromagnetic launch process is simulated in transient module with finite-element method coupling with the circuit. In this paper, a new improved configuration is added to the multistage appositional multipole coils. As shown in Fig. 1, the launch model is composed of three stage coils along the z-direction, and every stage coil in the $x-y$ plane is assembled with eight little pole coils. The next-stage coils are twisted an angle to the prior ones. It is called multistage twisty multipole field electromagnetic launcher. The radial section of the launcher barrel has the multipole magnetic field, and the axial space has a twisty magnetic field. As the projectile moves along the axial position of the launcher barrel, the multistage drive coils generate a twisty traveling magnetic wave along the launch direction. This helicoidal magnetic wave interacts with the projectile and produces axial acceleration force, azimuthal torsion force, and transverse restoring force. With huge axial thrust force, the projectile could be accelerated to high speed. The azimuthally torsion force makes the projectile obtain gyroscopic stabilization by a rotation around the thrust axis. Acted with the multipole small coils, the projectile maintains a dynamic balance with the transverse restoring force. As interaction of the rifled multipole magnetic wave, the projectile in free flight could keep the stabilization of the trajectory when leaving the launcher barrel.

Manuscript received June 8, 2011; revised August 23, 2011, October 9, 2011, and January 13, 2012; accepted February 8, 2012. Date of publication April 23, 2012; date of current version May 9, 2012. This work was supported by the Elitist Doctoral Dissertation Cultivated Foundation of Southwest Jiaotong University.

The authors are with the School of Electrical Engineering, Southwest Jiaotong University, Chengdu 610031, China (e-mail: zhu-yingwei@163.com; wangyu@swjtu.edu.cn; wrchen@swjtu.edu.cn; swjtu_yan@163.com; lihaitao840812@163.com).

Color versions of one or more of the figures in this paper are available online at http://ieeexplore.ieee.org.

Digital Object Identifier 10.1109/TPS.2012.2188530

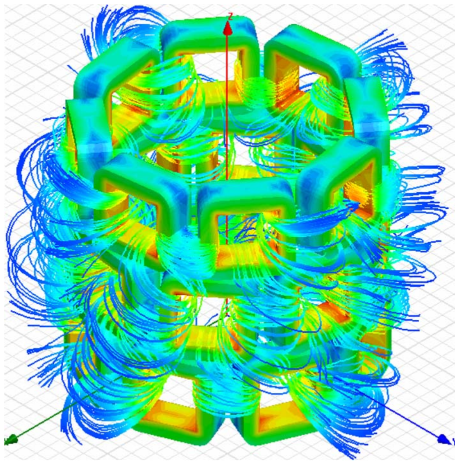

Fig. 2. Streamline of three-stage twisty magnetic octapole field.

II. Twisty Multipole Magnetic Field Configuration

Comparing with conventional straight solenoid coilguns, the multipole electromagnetic launcher has the radial magnetic field interacting with the loop eddy current of the projectile and produces a greater axial component of electromagnetic force to accelerate the projectile. For an improved performance and stability flight, we present a new multistage multipole electromagnetic launch configuration, and the next-stage pole coils are twisted an angle to the prior ones in sequence. As an example, in a three-stage twisty octapole field electromagnetic launcher, the twisted angle of every stage is 15°, and the pole coils could go back to the original size after three stages. These operations could generate a space periodic twisty magnetic field along the axis of the launcher barrel.

In the cross section of the barrel (in xy plane), it is the 2-D static magnetic n-pole field. As in the current-free regions, the Laplace's equation for the magnetic scalar potential is analyzed in the Appendix. In the twisted configuration, the magnetic scalar potential is also a function of z, and the magnetic field distribution has a helical and complicated component along the axial direction. With the electromagnetic field simulation software Ansoft Maxwell 3-D, the magnetic flux streamline of the three-stage twisty magnetic octapole field configuration is shown as in Fig. 2. It shows that the magnetic octapole field is twisted and the flux lines of a pole coil in one stage are coupling with another stage coil.

III. Power Circuit Consideration

One significant advantage of multistage multipole field electromagnetic launchers is that some pole coils are used as drive coil and could store much launch energy. The power supply and pole-coil connection have many choices. Pulsed capacitor banks and multiphase synchronous pulse generators are always used as power source [8], [9]. We propose the superconducting pulsed transformer used as the coilgun's current supplier [10]. By large inductance coil storing energy discharging to small inductance coil with transformer interaction, the drive coils could obtain transient and high pulsed current. The multipole coils have some types of electrical component arrangement. As an example, the two types of electrical component arrangement of magnetic octapole field electromagnetic launchers driven by pulsed capacitor banks are shown schematically in Fig. 3(a) and (b).

Fig. 3(a) shows the power circuit composed of the pulsed capacitor with electric charge source, continuous current diode, and octapole coils. The coil number starting from 11 means the first stage and the first pole coil. Eight pole coils are seriate in a clockwise direction. When the projectile reaches the suitable positions along the drive coils called discharge position, the displacement sensor detects it and controls the switch to turn on, and the pulsed capacitor discharges to multipole coils. Fig. 3(b) shows another coil arrangement type of power circuit mode. coil#11, coil#13, coil#15, and coil#17 are divided into single groups, and the others are divided into two groups. The adjacent coils are divided into different groups. Thus, the n-pole coils could be divided into much more groups. Each group coil is discharged with a pulsed capacitor source and could be fired with different discharge positions. The dividing group operation could reduce the drive coil inductance, relieve the power supply requirements, and make the magnetic traveling wave fine.

IV. Spinning Stability of Projectile

The first consideration of the multistage twisty multipole field electromagnetic launcher is the spinning stability of the projectile [11]–[17]. Because of the twisting operation, the next-stage coils are rotated with an angle to the prior ones. As the projectile moves along the axial position of the launcher barrel and the stage coils are fired with sequential scheduling, the multistage drive coils generate a twisty traveling magnetic wave. This helicoidal magnetic wave interacts with the induced eddy currents on the projectile, producing axial acceleration force, azimuthal torsion force, and transverse restoring force, as shown in Fig. 4. In particular, the azimuthal torsion force is huge and makes the projectile obtain gyroscopic stabilization by a rotation around the thrust axis. It is like the rifled guns, and the projectile in free flight could keep the stabilization of the trajectory when leaving the launcher barrel.

A. Inductive Eddy Current on Projectile

There are two main models for the numerical analysis of EML; they are based on the solution of an equivalent electric network or on the solution of the equations of the diffusion of the electromagnetic field [18]–[20]. The former focuses on calculating the mutual inductance between the drive coil and projectile. The eddy current distribution on the projectile is allowed to assume the form of a current filament or of a surface current. The central task of the field model is to resolve the magnetic field diffusion equation.

The electromagnetic launcher involves the interaction of the current density $\boldsymbol{J}$ of the projectile and the magnetic field $\boldsymbol{B}$ in the space

$$\boldsymbol{J} = \nabla \times \boldsymbol{B}/\mu_0 \quad (1)$$

where μ_0 is the permeability of the space.

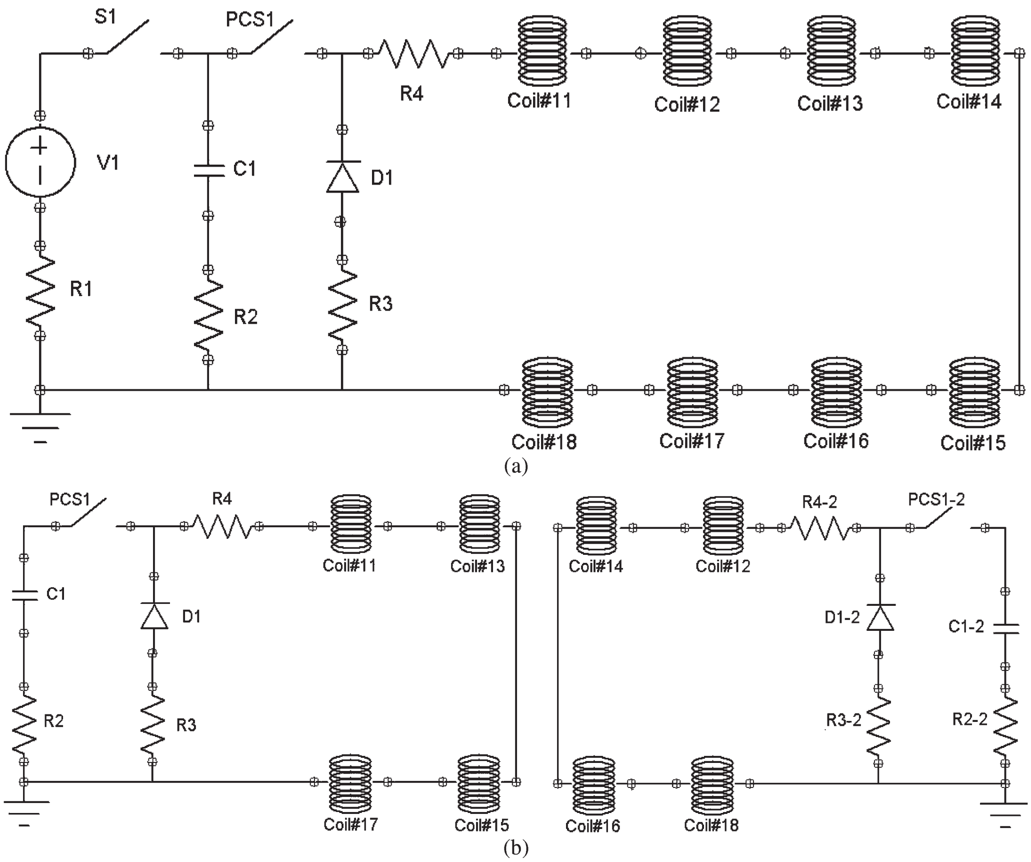

Fig. 3. Two types of electrical component arrangement of magnetic octapole field electromagnetic launchers. (a) All pole coils connected in series. (b) Pole coils divided into two groups.

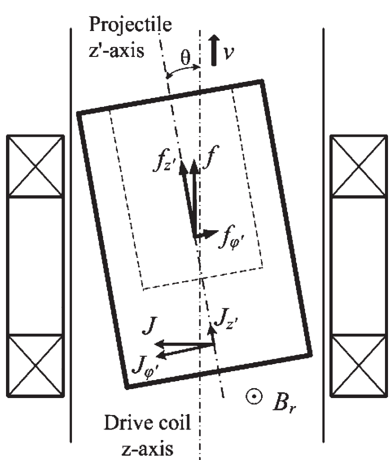

Fig. 4. Eddy current and magnetic force sketch on the projectile.

Using Faraday's law of induction and differential form of Ohm's law, we obtain the diffusion equation of the transient magnetic field permeating into a moving projectile

$$-\frac{\partial \boldsymbol{B}}{\partial t}+\nabla\times(\boldsymbol{v}\times\boldsymbol{B})=\nabla\times\boldsymbol{J}/\sigma=\nabla\times\nabla\times\boldsymbol{B}/(\sigma\mu_0) \quad (2)$$

where σ is the electric conductivity of projectile material and v is the speed of the moving projectile.

Additionally, the boundary conditions at the interface between the drive coil, projectile, and air spaces should be imposed on the solution of the magnetic field diffusion equation. With modern numerical calculation and finite-element method simulation, we could seek the solution of magnetic flux density with (2) and then substitute the solution in (1). The induced eddy current on the projectile could be obtained.

The skin effect of eddy current should also be considered; the skin depth is approximated by

$$\delta=\sqrt{\frac{2}{(\omega\sigma\mu_0\mu_r)}} \quad (3)$$

where ω is the source current's angular frequency, which is equal to $2\pi f$, σ is the projectile's conductivity, μ_r is the projectile's relative permeability, and μ_0 is the permeability of free space.

Because of the moving effect of the projectile, the current intensity in the end is greater than the head, as shown in Fig. 5. Every lateral face of the projectile has a quadrilateral eddy current distribution corresponding to the single small pole coil.

B. Axial Acceleration Force of Projectile

The main component of magnetic multipole field in the space is the radial direction, and the quadrilateral eddy current distribution on every lateral face of the projectile has axial and azimuthal components. Thus, the current density $\boldsymbol{J}$ on the

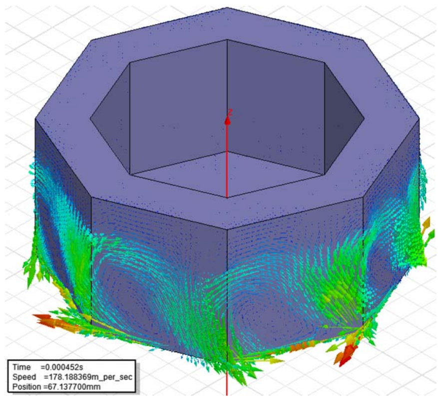

Fig. 5. Eddy current intensity distribution on the projectile.

projectile acting with magnetic field $\boldsymbol{B}$ produces the magnetic force density as

$$\begin{aligned}\boldsymbol{f} &= \boldsymbol{J} \times \boldsymbol{B} = f_r \boldsymbol{e}_r + f_\varphi \boldsymbol{e}_\varphi + f_z \boldsymbol{e}_z \\ &= (J_\varphi B_z - J_z B_\varphi)\boldsymbol{e}_r + (J_z B_r - J_r B_z)\boldsymbol{e}_\varphi \\ &\quad + (J_r B_\varphi - J_\varphi B_r)\boldsymbol{e}_z. \end{aligned} \tag{4}$$

Under the hypothesis of thin projectile, it is possible to assume $J_r \approx 0$, and furthermore in the domain of the projectile, the magnetic flux density can be assumed as directed in the radial direction.

The axial acceleration force of the projectile is

$$f_z = -J_\varphi B_r \quad F_z = \int_V f_z dV \tag{5}$$

where J_φ is the azimuthal component current density on the projectile, B_r is the radial component magnetic flux density, and V is the volume of the projectile.

The axial acceleration force of the projectile is the main component of electromagnetic force to accelerate the projectile to high speed.

The z component motion equations of the projectile are

$$a_z = \frac{F_z}{m} = \int_V J_\varphi B_r dV/m \tag{6}$$

$$v_z = v_0 + \int_0^T a_z dt \tag{7}$$

$$s_z = s_0 + \int_0^T v_z dt \tag{8}$$

where a_z is the acceleration of the projectile, m is the mass of the projectile, v_0 is the initial (or injection) speed of the projectile, v_z is the final speed, s_0 is the initial position of the projectile, and s_z is the final position.

C. Azimuthal Torsion Force of Projectile

The azimuthal component force of the projectile is

$$f_\varphi = J_z B_r \quad F_\varphi = \int_V f_\varphi dV \tag{9}$$

where J_z is the axial component current density and B_r is the radial component magnetic flux density.

Acted with the azimuthal component force, the projectile has an axial torque as

$$m_z = r f_\varphi = r J_z B_r \quad M_z = \int_V m_z dV \tag{10}$$

where m_z is the axial component torque and r is the projectile radius.

Because of the twisty magnetic field and the projectile's moving effect, the composition of azimuthal torsion forces does not equal zero. The axial torque makes the projectile have a rotational motion about its axis. That is called spinning which makes the projectile fly stability like a rifle.

The rotational motion equations of the projectile about the z-axis are

$$\alpha_z = M_z/I_z = \int_V r J_z B_r dV/I_z \tag{11}$$

$$\omega_z = \omega_0 + \int_0^T \alpha_z dt \tag{12}$$

$$\theta_z = \theta_0 + \int_0^T \omega_z dt \tag{13}$$

where α_z is the angular acceleration of the projectile, I_z is the moment of inertia with respect to the z-axis, ω_0 is the initial angular velocity of the projectile, ω_z is the final velocity, θ_0 is the initial angle position of the projectile, and θ_z is the final angle position.

D. Transverse Force and Position of Projectile

The radial component force of the projectile is

$$f_r = J_\varphi B_z - J_z B_\varphi \quad F_r = \int_V f_r dV \tag{14}$$

where B_z, B_φ are the axial and the azimuthal component magnetic flux density, f_r is the radial component force, and resultant force F_r is the transverse force of the projectile.

As the axial and azimuthal component magnetic flux densities are much little, the radial component force is much less than the axial component force. Sometimes, the projectile's axis is not always in coaxial position with the barrel. An uneven distribution of radial forces can produce transverse motion, even oscillations around the projectile mass center. However, the inductive eddy counteractive causes a restoring force in the opposite direction of the deviation.

E. Energy Conversion Efficiency

As the launcher is driven by the pulsed capacitor banks, the system energy conversion efficiency is the ratio of the

TABLE I
SOME PERTINENT PARAMETERS OF SIMULATION MODEL

Structure	Parameter	Value
Octapole coils	Material	Copper
	Inner section	30mm×30mm
	Outer section	60mm×60mm
	Length	20mm
	Turns	30
	Total Inductance	292.44μH
	Barrel caliber	73mm
	Twisted angle	15deg
Projectile	Material	Aluminum
	Inner radius	51mm
	Outer radius	71mm
	Length	60mm
	Mass	1.52kg
	Initial speed	10m/s
Capacitor banks	First stage	1000μF, 20kV
	Second stage	400μF, 32kV
	Third stage	200μF, 45kV
Discharge position	First stage	-25mm
	Second stage	-26mm
	Third stage	-27mm

projectile's kinetic energy increment to the electrical energy initially stored in the capacitor. The efficiency is expressed by

$$\eta = \frac{\Delta E_k}{E_{C0}} = \frac{\frac{1}{2}m\left(v_z^2 - v_0^2\right) + \frac{1}{2}I_z\omega_z^2}{\sum_N \frac{1}{2}CU_{C0}^2} \tag{15}$$

where N is the launch stage number and U_{C0} is the initial voltage of the charged capacitor.

V. NUMERIC SIMULATION EVALUATION

This section presents the simulation results and performance evaluation of a three-stage twisty octapole field electromagnetic launcher discussed in the previous content. In order to analyze the spinning motion of the projectile, we select Infolytica MagNet to implement such a 3-D transient motion simulation. Infolytica MagNet is the leading international simulation software of electrical engineering, particularly in motion simulations with multiple degrees of freedom. MagNet's analysis of electromagnetic models is based upon the finite-element method. The finite-element mesh can be refined through subdivision (h-type adaption) or by increasing their polynomial order (p-type adaption). The 3-D transient motion solver adopts the advanced T-Omega equations. Time adaption estimates an appropriate time step length at each step of the solution. Solution accuracy is influenced by the following factors: mesh refinement, polynomial order, boundary conditions, CG tolerance, maximum Newton iterations, and Newton tolerance. Nonlinear problems can be solved using the Newton–Raphson method or the successive substitution method.

Some pertinent parameters of the three-stage twisty octapole field electromagnetic launcher are given in Table I. All the octapole coils are of the same structure. We set the next-stage pole coils to twist 15° to the prior ones in sequence, and the fourth-stage pole coils could return to original size. The 1.52-kg projectile is a hollow prism with octagonal cross section in accord with the octapole driving coils. The radii are of the circumcircle of the octagonal model. The projectile's initial speed of 10 m/s could be attained with a catapult coil as in [7]. As we consider the thickness of the flyway tube, the radial gap distance between the projectile and the barrel is set to 2 mm. The type (a) of circuit in Fig. 3 is used to generate the performance simulations. The firing sequence of the capacitors is determined by the discharge position defined as the axial distance between the midsections of the stage coils to the projectile rears. The first-stage discharge position of the projectile is -25 mm. As the entrance speed of the projectile is gradually increased in each stage, the parameters of the capacitor banks and the discharge position have been adapted to adjustment to improve the launch efficiency. For considering the displacement in transverse motion, we set the gravity in the y-direction.

Figs. 6–12 show the numerical simulation results of the three-stage twisty octapole field electromagnetic launcher. As indicated in the figures, a 1.52-kg projectile accelerated to an exit velocity of 119.13 m/s has been achieved, and the magnetic torque profile shows an impressive demonstration of spinning.

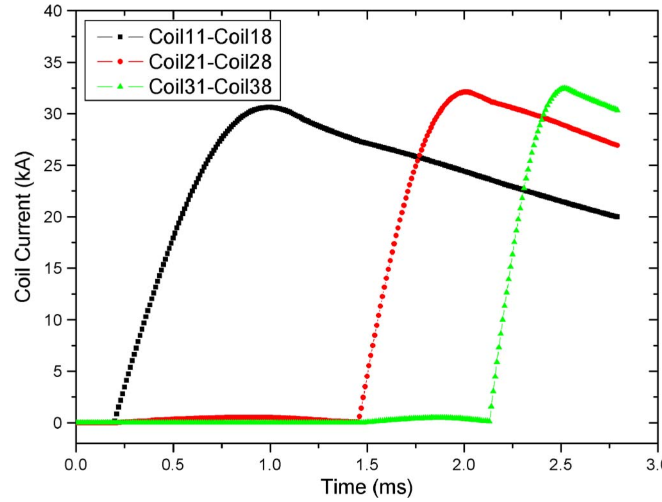

Fig. 6. Running currents in every stage coil as a function of launch time.

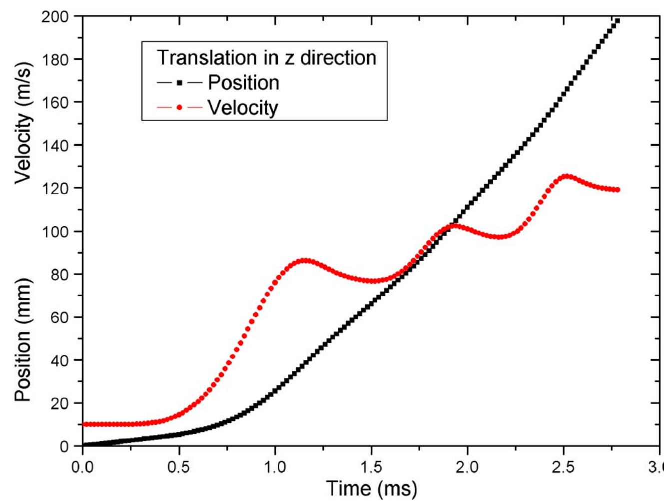

Fig. 7. Projectile velocity and position of translation in z-direction.

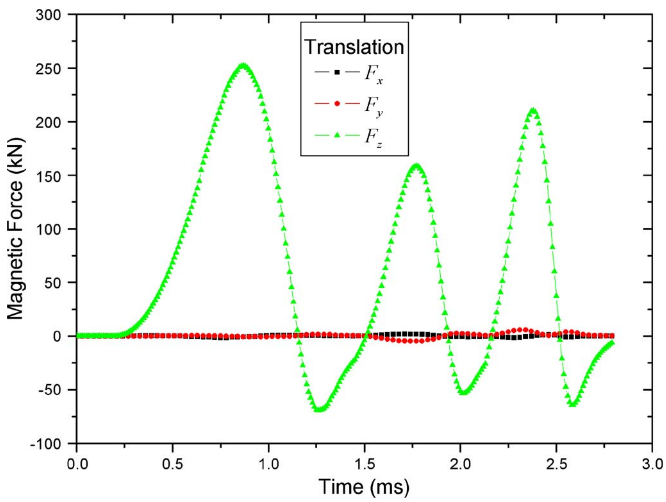

Fig. 8. Magnetic force profiles of translation in xyz-direction.

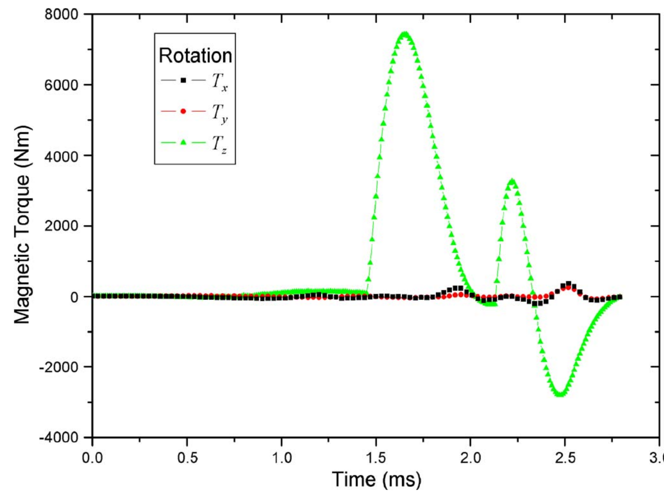

Fig. 9. Axial torque profiles of rotation about xyz-axis.

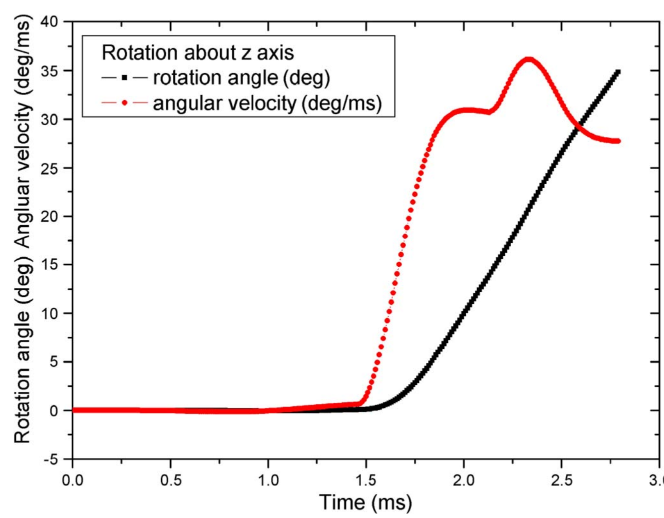

Fig. 10. Rotation angle and angular velocity profiles about z-axis.

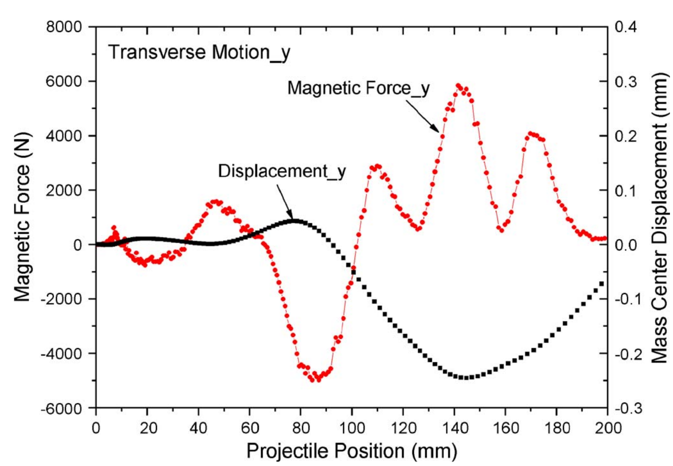

Fig. 11. Magnetic force and displacement of transverse motion in y-direction.

The running currents in every stage coil are shown in Fig. 6 as a function of launch time. The peak currents of coils are round about 32 kA, and the current rise time reduces from 0.8 to 0.38 ms.

Fig. 7 shows the projectile's velocity and position of translation in the z-direction. It indicates that the 1.52-kg projectile is accelerated to 119.13 m/s in a 200-mm displacement during the time of 2.8 ms. The velocity curve is fluctuating because of the braking effect in axial acceleration [21].

The resulting magnetic force profiles of translation in xyz-directions are shown in Fig. 8. The component F_z of magnetic force is much larger than the F_x and F_y. The maximal F_z of three positive pinnacles is 252.1 kN. The components F_x and F_y are nearly zero. These indicate that the axial component of electromagnetic force is much greater and the radial force acts as restoring effect. The profile also shows three negative troughs called brake force due to the eddy current of the projectile in reverse. In order to avoid the braking effect, the pulsed current profile of the drive coil should match the mutual inductance gradient as the projectile moves.

Because of the symmetry of the appositional coil arrangement, theoretical analysis and numerical results indicate that the axial torque of the appositional coil launcher approaches to zero. Fig. 9 illustrates the axial torque profiles of rotational motion about the xyz-axis as a function of launch time in the barrel. It is indicated that the maximal magnetic torque of $7427.15\ \mathrm{N} \cdot \mathrm{m}$ is in the z-direction and other direction torques are small. That is an impressive torsion of the projectile acted with drive coils. This validates the spinning motion of the projectile in the twisty multipole field electromagnetic launch.

The rotation angle and angular velocity profiles of the projectile about the z-axis are shown in Fig. 10 as a function of launch time. The resulting rotation angle is 34.85°, and the angular velocity is $27.71^\circ/\mathrm{ms}$. These are the obvious proofs of spinning motion of the projectile in the launch process.

Fig. 11 shows the magnetic force and position of transverse translation in the y-direction as a function of projectile position. The magnetic force and transverse motion are opposite every time. F_y has a little fluctuant because of the restoring force against the gravity of the projectile in the y-direction. The maximal value of F_y is 5836.1 N, and the maximal value of s_y is 0.246 mm. It is indicated that the transverse displacement is much littler than the radial gap distance of 2 mm between the projectile and the flyway tube. F_y applied on the projectile has an opposite sign with respect to s_y, thus indicating a

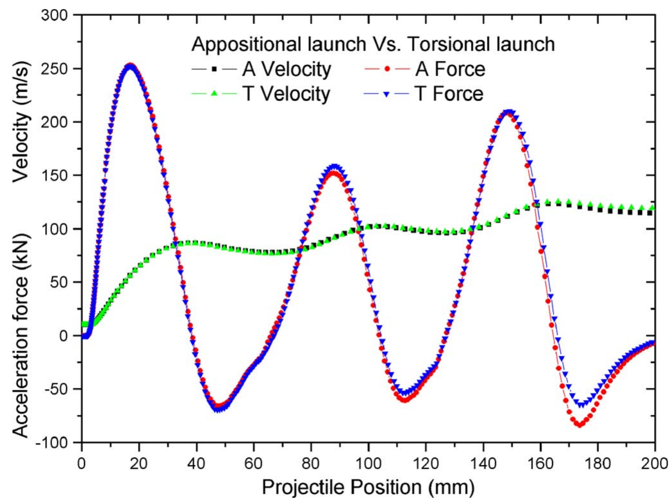

Fig. 12. Comparison of acceleration force and velocity in z-direction of torsional launch versus appositional launch.

suspension effect of the projectile in motion. Because of the symmetry of the device, a similar behavior is expected along the x-direction.

As a comparison of torsional coil launch with appositional coil launch, the resulting velocity and acceleration force profiles in the z-direction are shown in Fig. 12 as a function of projectile position in the barrel. It is indicated that the torsion option of the multistage coil launcher makes little influence on axial acceleration force and exit velocity. Adding the projectile's angular kinetic energy, the energy efficiency of the proposed launcher is bigger than the standard with 3-D calculations.

VI. Conclusion

This paper has presented a theoretical analysis and numerical evaluation of a three-stage twisty octapole field electromagnetic launcher. Power supply module for the pole coils divided into groups has been considered. The electromagnetic force analysis of projectile dynamics indicates that the multistage twisty multipole field waves make the projectile involved in axial translation and rotation that keep the projectile fly stability. Numeric simulation results of the three-stage twisty octapole field electromagnetic launcher indicate that the magnetic torque of rotational motion is impressively large and the transverse displacement of the projectile is very small. Compared with the appositional configuration, the torsion option of the multistage coil launcher makes little influence on axial acceleration force and exit velocity. We are working on the design and fabrication of an experimental launch model.

The multistage twisty multipole field electromagnetic launcher has the advantages of huge thrust force, large driven mass, reliable spinning stability, suspension restoring force, and high-speed launch. We suggest that this launch mode could be applied in the evacuated tube transportation vehicle, tunnel boring machine, and spacecraft propulsion launcher [22]–[24].

Appendix

Considering that the drive coils are excited with constant current, it is the 2-D static magnetic n-pole field in the cross section of the barrel (in xy plane). The current sources are directed along the z-axis, while the azimuth currents (required to close the current loop) are at $z = +\infty$ and $z = -\infty$. As in the current-free regions and without source term, the Laplace's equation for the magnetic scalar potential in Cartesian coordinate system is

$$\frac{\partial^2\phi}{\partial x^2} + \frac{\partial^2\phi}{\partial y^2} = 0 \tag{1a}$$

where ϕ is the magnetic scalar potential at the air region.

Define ϕ_n as the magnetic scalar potential of the n-pole field, $n = 2, 4, 6 \ldots$. The solution of the Laplace harmonic equation is given by a polynomial expression as

$$\phi_n = a_{m0}x^m + a_{m-1,1}x^{m-1}y + a_{m-2,2}x^{m-2}y^2 + \ldots + a_{0m}y^m. \tag{2a}$$

Defining $m = n/2$, $\partial^{(m-1)}H_y/\partial x^{(m-1)} = H_N^{(m-1)} = b_{mN}$ as the vertical n-pole field and, $\partial^{(m-1)}H_x/\partial x^{(m-1)} = H_s^{(m-1)} = b_{mS}$ as the oblique n-pole field, we could obtain the formal solution

$$\phi_n = -\frac{1}{m!}\left[b_{ms}\sum_{i=0}^{M_1}(-1)^i C_m^{2i} x^{m-2i}y^{2i} + b_{mN}\sum_{i=0}^{M_2}(-1)^i C_m^{2i+1}x^{m-2i-1}y^{2i+1}\right] \tag{3a}$$

where $M_1 = m/2$ and $M_2 = M_1 - 1$, as m is an even number; if m is an odd number, then $M_2 = M_1 = (m-1)/2$.

As the n-pole coils twisted with the axis of the launcher barrel, we resolve the formal solution in cylindrical coordinate system

$$x = r\cos(\theta); \quad y = r\sin(\theta); \quad z = z. \tag{4a}$$

Half-angle formulas are expressed in series as

$$\cos m\theta = \sum_{i=0}^{M_1}(-1)^i C_m^{2i}\cos^{(m-2i)}\theta\sin^{2i}\theta \tag{5a}$$

$$\sin m\theta = \sum_{i=0}^{M_2}(-1)^i C_m^{2i+1}\cos^{(m-2i-1)}\theta\sin^{(2i+1)}\theta. \tag{6a}$$

Taking the above two formulas into (3a), the equation is therefore

$$\phi_n = -\frac{r^m}{m!}(b_{mS}\cos m\theta + b_{mN}\sin m\theta). \tag{7a}$$

Thus, the magnetic field intensity of the m-rank harmonic wave in the air region is

$$H_{rn}(r,\theta) = -\frac{\partial\phi_n}{\partial r} = \frac{r^{m-1}}{(m-1)!} \times (b_{mS}\cos m\theta + b_{mN}\sin m\theta) \tag{8a}$$

$$H_{\theta n}(r,\theta) = -\frac{1}{r}\frac{\partial\phi_n}{\partial\theta} = \frac{r^{m-1}}{(m-1)!} \times (b_{mN}\cos m\theta - b_{mS}\sin m\theta). \tag{9a}$$

Twisting the single-group pole coils with an angle δ, the magnetic flux density of the n-pole m-rank harmonic wave in static field is

$$B_{rn}(r,\theta) = \frac{\mu_0 r^{m-1}}{(m-1)!}\left[b_{mS}\cos m(\theta+\delta) + b_{mN}\sin m(\theta+\delta)\right] \tag{10a}$$

$$B_{\theta n}(r,\theta) = \frac{\mu_0 r^{m-1}}{(m-1)!}\left[b_{mN}\cos m(\theta+\delta) - b_{mS}\sin m(\theta+\delta)\right]. \tag{11a}$$

The twisted n-pole field distribution related to the solution by (10a) and (11a) should be reported together with the imposition of the boundary conditions for the determination of the coefficients of the given expansion of the magnetic scalar potential.

REFERENCES

[1] W. Ying, R. A. Marshall, and C. Shukang, *Physics of Electric Launch*. Beijing, China: Science Press, 2004.

[2] I. R. McNab, "Early electric gun research," *IEEE Trans. Magn.*, vol. 35, no. 1, pp. 250–261, Jan. 1999.

[3] H. D. Fair, "Progress in electromagnetic launch science and technology," *IEEE Trans. Magn.*, vol. 42, no. 1, pp. 93–98, Jan. 2007.

[4] H. D. Fair, "Advances in electromagnetic launch science and technology and its applications," *IEEE Trans. Magn.*, vol. 45, no. 1, pp. 225–230, Jan. 2009.

[5] P. G. Rutberg, G. A. Shvetsov, and I. I. Kumkova, "New steps in EML research in Russia," *IEEE Trans. Magn.*, vol. 45, no. 1, pp. 231–236, Jan. 2009.

[6] I. R. McNab, "Progress on hypervelocity railgun research for launch to space," *IEEE Trans. Magn.*, vol. 45, no. 1, pp. 381–388, Jan. 2009.

[7] Y. Zhu, Y. Wang, Z. Yan, L. Dong, X. Xie, and H. Li, "Multipole field electromagnetic launcher," *IEEE Trans. Magn.*, vol. 46, no. 7, pp. 2622–2627, Jul. 2010.

[8] J. He, E. Levi, Z. Zabar, and L. Birenbaum, "Concerning the design of capacitively driven induction coil guns," *IEEE Trans. Magn.*, vol. 17, no. 3, pp. 429–438, Jun. 1989.

[9] R. J. Kaye, "Operational requirements and issues for coilgun electromagnetic launchers," *IEEE Trans. Magn.*, vol. 41, no. 1, pp. 194–199, Jan. 2005.

[10] A. Sitzman, D. Surls, and J. Mallick, "Design, construction, and testing of an inductive pulsed-power supply for a small railgun," *IEEE Trans. Magn.*, vol. 43, no. 1, pp. 270–274, Jan. 2007.

[11] K. B. Kim, Z. Zabar, E. Levi, and L. Birembaum, "In-bore projectile dynamics in the linear induction launcher (LIL), Part I: Oscillations," *IEEE Trans. Magn.*, vol. 31, no. 1, pp. 484–488, Jan. 1995.

[12] K. B. Kim, Z. Zabar, E. Levi, and L. Birembaum, "In-bore projectile dynamics in the linear induction launcher (LIL), Part II: Balloting, spinning, and nutation," *IEEE Trans. Magn.*, vol. 31, no. 1, pp. 489–492, Jan. 1995.

[13] I. R. Shokair, "Projectile transverse motion and stability in electromagnetic induction launchers," *IEEE Trans. Magn.*, vol. 31, no. 1, pp. 504–509, Jan. 1995.

[14] A. Musolino, M. Raugi, and B. Tellini, "3-D field analysis in tubular induction launcher with armature transverse motion," *IEEE Trans. Magn.*, vol. 35, no. 1, pp. 154–159, Jan. 1999.

[15] S. Barmada, A. Musolino, M. Raugi, and R. Rizzo, "Analysis of the performance of a multi-stage pulsed linear induction launcher," *IEEE Trans. Magn.*, vol. 37, no. 1, pp. 111–115, Jan. 2001.

[16] G. Becherini, "Gyroscopic stabilization of launch package in induction type coilgun," *IEEE Trans. Magn.*, vol. 37, no. 1, pp. 116–122, Jan. 2001.

[17] G. Becherini and B. Tellini, "Helicoidal electromagnetic field for coilgun armature stabilization," *IEEE Trans. Magn.*, vol. 39, no. 1, pp. 108–111, Jan. 2003.

[18] L. Shoubao, R. Jiangjun, P. Ying, Z. Yujiao, and Z. Yadong, "Improvement of current filament method and its application in performance analysis of induction coil gun," *IEEE Trans. Plasma Sci.*, vol. 39, no. 1, pp. 382–389, Jan. 2011.

[19] S. Aksoy, A. Balikci, Z. Zabar, and L. Birenbaum, "Numerical investigation of the effect of a longitudinally layered armature on coilgun performance," *IEEE Trans. Plasma Sci.*, vol. 39, no. 1, pp. 5–8, Jan. 2011.

[20] S. Aksoy, M. F. Yavuz, and A. Balikci, "Transient modeling of a linear induction launcher type coil gun with two dimensional cylindrical FDTD method," *IET Elect. Power Appl.*, vol. 5, no. 1, pp. 153–158, Jan. 2011.

[21] Y. Zhang, J. Ruan, Y. Wang, Z. Du, S. Liu, and Y. Zhang, "Performance improvement of a coil launcher," *IEEE Trans. Plasma Sci.*, vol. 39, no. 1, pp. 210–214, Jan. 2011.

[22] B. D. Skurdal and R. L. Gaigler, "Multimission electromagnetic launcher," *IEEE Trans. Magn.*, vol. 45, no. 1, pp. 458–461, Jan. 2009.

[23] L. Li, M. Ma, B. Kou, and Q. Chen, "Analysis and design of moving-magnet-type linear synchronous motor for electromagnetic launch system," *IEEE Trans. Plasma Sci.*, vol. 39, no. 1, pp. 121–126, Jan. 2011.

[24] M. R. Wright, S. B. Kuznetsov, and K. J. Kloesel, "A lunar electromagnetic launch system for in situ resource utilization," *IEEE Trans. Plasma Sci.*, vol. 39, no. 1, pp. 521–528, Jan. 2011.

Zhu Yingwei was born in Hubei Province, China, on October 5, 1982. He received the B.S. degree in electronic science and technology and the Ph.D. degree in theory of electrical engineering and new technology from Southwest Jiaotong University, Chengdu, China, in 2006 and 2011, respectively.

He is currently a Teacher with the School of Electrical Engineering and Information, Sichuan University, Chengdu. His major fields of research interests include electromagnetic launch technology and electromagnetic-field numerical simulation.

Wang Yu was born in Henan Province, China, on November 7, 1960. He received the Ph.D. degree in physical electronics from the Huazhong University of Science and Technology, Wuhan, China, in 2001.

He is currently a Professor with the School of Electrical Engineering, Southwest Jiaotong University, Chengdu, China. His research interests include superconducting electrotechnics and material technology.

Chen Weirong was born in Sichuan Province, China, on January 2, 1965. He received the Ph.D. degree in electrification and robotization of rail traction from Southwest Jiaotong University (SWJTU), Chengdu, China, in 1998.

He is currently a Professor with the School of Electrical Engineering, SWJTU. His research interests include SCADA system, power system, and artificial intelligence.

Yan Zhongming was born in Zhejiang Province, China, on July 12, 1982. He received the M.S. degree in electrical engineering from Southwest Jiaotong University, Chengdu, China, in 2007, where he is currently working toward the Ph.D. degree in theory of electrical engineering and new technology.

His research interests include superconducting electromotor and numerical analysis of electromagnetic fields.

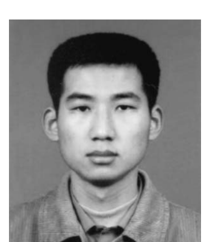

Li Haitao was born in Shandong Province, China, on September 7, 1984. He received the B.S. degree in electrical engineering from the Shandong University of Technology, Zibo, China, in 2007, where he is currently working toward the Ph.D. degree in theory of electrical engineering and new technology.

He is currently with the School of Electrical Engineering, Southwest Jiaotong University, Chengdu, China. His research interests include pulsed power technology and its applications.